Stability and plasticity of intrinsic membrane properties in hippocampal CA1 pyramidal neurons: effects of internal anions

Catherine Cook Kaczorowski[1,2], John Disterhoft[2] and Nelson Spruston[1]

[1]*Northwestern University, Department of Neurobiology and Physiology, Evanston, IL, USA*
[2]*Northwestern University Feinberg School of Medicine, Department of Physiology, Chicago, IL, USA*

CA1 pyramidal neurons from animals that have acquired hippocampal tasks show increased neuronal excitability, as evidenced by a reduction in the postburst afterhyperpolarization (AHP). Studies of AHP plasticity require stable long-term recordings, which are affected by the intracellular solutions potassium methylsulphate (KMeth) or potassium gluconate (KGluc). Here we show immediate and gradual effects of these intracellular solutions on measurement of the AHP and basic membrane properties, and on the induction of AHP plasticity in CA1 pyramidal neurons from rat hippocampal slices. The AHP measured immediately after establishing whole-cell recordings was larger with KMeth than with KGluc. In general, the AHP in KMeth was comparable to the AHP measured in the perforated-patch configuration. However, KMeth induced time-dependent changes in the intrinsic membrane properties of CA1 pyramidal neurons. Specifically, input resistance progressively increased by 70% after 50 min; correspondingly, the current required to trigger an action potential and the fast after-depolarization following action potentials gradually decreased by about 50%. Conversely, these measures were stable in KGluc. We also demonstrate that activity-dependent plasticity of the AHP occurs with physiologically relevant stimuli in KGluc. AHPs triggered with theta-burst firing every 30 s were progressively reduced, whereas AHPs elicited every 150 s were stable. Blockade of the apamin-sensitive AHP current (I_{AHP}) was insufficient to block AHP plasticity, suggesting that plasticity is manifested through changes in the apamin-insensitive slow AHP current (sI_{AHP}). These changes were observed in the presence of synaptic blockers, and therefore reflect changes in the intrinsic properties of the neurons. However, no AHP plasticity was observed using KMeth. In summary, these data show that KMeth produces time-dependent changes in basic membrane properties and prevents or obscures activity-dependent reduction of the AHP. In whole-cell recordings using KGluc, repetitive theta-burst firing induced AHP plasticity that mimics learning-related reduction in the AHP.

(Resubmitted 7 November 2006; accepted 22 November 2006; first published online 23 November 2006)
Corresponding author C. C. Kaczorowski: N. Spruston, Department of Neurobiology and Physiology, 2205 Tech Drive, Evanston, IL, 60208, USA. Email: spruston@northwestern.edu

The hippocampus is crucial for the formation of declarative memories, as observed by deficits in human patients with temporal lobe damage (Milner & Penfield, 1955; Scoville & Milner, 1957). Furthermore, damage restricted to the CA1 region of the hippocampus is sufficient to produce similar, albeit less severe, memory deficits (Zola-Morgan *et al.* 1986; Rempel-Clower *et al.* 1996).

The majority of pyramidal neurons in the CA1 region in rabbit and rat exhibit a learning-related enhancement in neuronal excitability *in vivo* (Berger & Thompson, 1978; McEchron & Disterhoft, 1997; McEchron *et al.* 2001) and *in vitro* (Disterhoft *et al.* 1986; Moyer *et al.* 1996, 2000; Oh *et al.* 2003; Zelcer *et al.* 2006). A reduction in the post-burst afterhyperpolarization (AHP) has been proposed as a general mechanism that underlies these changes in neuronal excitability and hippocampus-dependent learning observed *in vivo* (for review see Disterhoft *et al.* 2004).

Activity-dependent changes in neuronal excitability have been studied in multiple cell types *in vitro* (Aizenman & Linden, 2000; Cudmore & Turrigiano, 2004; Fan *et al.* 2005). In an effort to understand how neuronal activity patterns that are observed during learning can

 DOI: 10.1113/jphysiol.2006.124586

produce a reduction in the AHP, we sought to identify a stimulation protocol that reduces the AHP in CA1 neurons in acute brain slices. Previous studies have shown that high-frequency bursts of action potentials (Kandel & Spencer, 1961; Ranck, 1973) delivered at theta frequency (theta-burst firing) are observed *in vivo* during learning (Otto *et al.* 1991) and are effective at inducing long-term potentiation (LTP) of synaptic transmission (Larson *et al.* 1986; Thomas *et al.* 1998). Therefore, we hypothesized that repetitive theta-burst firing of CA1 neurons may increase neuronal excitability by reducing the AHP.

In order to effectively study plasticity of the AHP *in vitro*, a recording environment is required in which the physiological characteristics of the neuron are conserved and maintained for long periods of time. However, maintaining a stable whole-cell recording is difficult because dialysis of the cell with internal pipette solution can affect the electrophysiological characteristics of the neuron (Kay, 1992). There are multiple reports demonstrating effects of the main internal anion on the electrical characteristics of several different types of neurons (McKillen *et al.* 1994; Nakajima *et al.* 1992; Robbins *et al.* 1992; Schwindt *et al.* 1992; Spigelman *et al.* 1992). In addition, the main internal anion has a major impact on neuronal stability, partly through its propensity to stabilize both proteins and the membrane (Tasaki *et al.* 1965; Inoue *et al.* 1976; Collins & Washabaugh, 1985). Lastly, time-dependent effects of the internal anion on the amplitude and activation rate of delayed rectifier K^+ current (I_K) have been shown to develop progressively over 50 min (Adams & Oxford, 1983). Although the effects of internal anions on the electrical characteristics of CA1 pyramidal neurons have been characterized following dialysis (Velumian *et al.* 1997; Zhang *et al.* 1994), these studies did not distinguish between immediate (at rupture) and gradual effects of the internal solution on the AHP or basic membrane properties.

We were interested in determining which intracellular solution, potassium methylsulphate (KMeth) or potassium gluconate (KGluc), used in the whole-cell patch-clamp configuration, produces an AHP that best matches the AHP measured when the internal milieu is undisturbed. Previous studies demonstrated that the AHP measured using sharp-microelectrode recordings was best reproduced in whole-cell recordings using KMeth. However, it remains unclear whether or not recordings with sharp-microelectrodes filled with KMeth are the best standard for the AHP *in vivo* (Velumian *et al.* 1997; Zhang *et al.* 1994).

Furthermore, we set out to examine the effects of KMeth and KGluc on the stability of the basic membrane properties, as well as the plasticity of the AHP induced with various stimulation protocols. Preliminary reports have been published in abstract form (Kaczorowski *et al.* 2002, 2003).

Methods

Transverse hippocampal slices and internal solutions

All animal procedures were approved by the Northwestern University Animal Care and Use Committee. We used male Wistar rats at postnatal day 14–28, unless otherwise noted. Under deep halothane anaesthesia, the rat was decapitated and the brain quickly removed and placed into ice-cold artificial cerebral spinal fluid (aCSF) containing (mM): NaCl 125, glucose 25, $NaHCO_3$ 25, KCl 2.5, NaH_2PO_4 1.25, $CaCl_2$ 2, $MgCl_2$ 1; pH 7.5, bubbled with 95% O_2–5% CO_2. A blocking cut was made to obtain near-horizontal slices, which maintain intact CA1 apical dendrites within the hippocampal slice. Slices (300 μm) of the medial hippocampus and adjacent cortex were made using a Leica vibratome (Wetzlar, Germany). The slices were first incubated at 34°C in bubbled aCSF for 30 min, and then incubated at room temperature (22°C) in bubbled aCSF for 1–4 h before use.

For whole-cell and perforated-patch recordings, electrodes prepared from thin-walled capillary glass were filled with either 115 mM potassium methylsulphate- or 115 mM potassium gluconate-based internal solution (KMeth or KGluc, respectively) and had a resistance of 2–4 MΩ. Both solutions also contained (mM): KCl 20, sodium phosphocreatine 10, HEPES 10, MgATP 2 and NaGTP 0.3, and 0.10% biocytin; pH was adjusted to 7.3 with KOH. For perforated-patch recordings, electrodes were prepared in the same manner, but back-filled with a solution containing 5 μl Amphotericin B (1 mg in 50 μl distilled and deionized H_2O and sonicated for 5 min) dissolved into 1 ml of either KMeth or KGluc. Unless otherwise stated, chemicals were obtained from Sigma (St Louis, MO, USA). Potassium methylsulphate was purchased from ICN Biomedicals Inc. (Aurora, OH, USA).

Electrophysiological recording

Slices were transferred to a recording chamber mounted on a Zeiss Axioskop (Oberkochen, Germany) where they were submerged in oxygenated aCSF at 33–34°C. Neurons were visualized with infrared differential video interference microscopy. High-resistance seals (> 1 GΩ) were obtained under visual control on the somata of CA1 pyramidal neurons and brief suction was applied to the patch in order to gain whole-cell access to the neuron. For perforated-patch recordings, high resistance seals (> 1 GΩ) were obtained and the seal and access resistance was monitored every 5–20 s to verify a steady gain of access, indicative of perforated-patch configuration. The fact that internal anion effects were not observed indicated that spontaneous rupture did not occur during perforated-patch recordings.

Once in whole-cell or perforated-patch configuration, cells were evaluated on a number of criteria and accepted for use only if they had a resting membrane potential (V_m) < -58 mV, access resistance (R_s) < 40 MΩ, input resistance (R_N) > 30 MΩ and an action potential amplitude > 70 mV relative to action potential threshold (see below). Most recordings were performed in the current-clamp mode using a Dagan current-clamp amplifier; cells were held at -66 mV by manually adjusting the holding current (< -100 pA). In one set of experiments, a Multiclamp 700B (Molecular Devices, Sunnyvale, CA, USA) was used to perform both current-clamp and voltage-clamp recordings in the same neuron ($R_s < 10$ MΩ). The electrode capacitance and series resistance (R_s) were monitored, compensated and recorded frequently throughout the duration of the recording. No leak subtraction was performed in the voltage-clamp experiments. In all experiments, $GABA_A$ receptors, ionotropic glutamate receptors and muscarinic acetylcholine receptors were blocked by the addition of SR95531 (2 mM), kynurenic acid (2 mM) and atropine (1 μM) to the standard aCSF solution, respectively. In a subset of experiments, a stock solution of apamin (0.1 mM) was prepared from a 5% acetic acid solution and stored at -20°C frozen for up to 3 days. Apamin was diluted with aCSF to a final bath concentration of 100 nM on the day of use. aCSF used for control comparisons contained an equal proportion of acetic acid. Noradrenaline and $CdCl_2$ were dissolved in distilled and deionized water and prepared fresh daily.

Stimulation and recording protocols

In order to assess the immediate effects of KMeth and KGluc, AHPs and membrane properties were measured directly after establishing a whole-cell recording. Comparisons with perforated-patch recordings were made to determine which internal solution best preserved the AHP observed under more physiological conditions. In these experiments, AHPs were triggered by two distinct stimulation protocols. First, we used a conventional high-frequency train of action potentials that consisted of 50 action potentials at 50 Hz. Second, we used theta-burst firing that consisted of 10 bursts of five action potentials triggered using brief (2 ms) somatic current injections (1 nA) at 100 Hz with an interburst frequency of 5 Hz. AHPs were elicited by alternating between theta-burst firing and 50 Hz firing, and were reported as an average of two to three sweeps per cell.

In order to assess the gradual effects of the internal solution on the AHP independent of activity-induced changes, we used a low-activity protocol in whole-cell recordings made with either KMeth or KGluc (Fig. 1*A*). In this protocol, an AHP was elicited using theta-burst firing once every 150 s, resulting in a total of 40 action potentials per 5 min, for up to 1 h. Theta-burst firing consisted of four bursts of five action potentials triggered using brief (2 ms) somatic current injections (1 nA) at 100 Hz with an interburst frequency of 5 Hz (Fig. 1*Ba*). The somatic current injection was set at +1 nA to ensure faithful generation of action potentials with reproducible timing.

The gradual effects of the KMeth- and KGluc-based internal solutions on basic membrane properties and the fast afterdepolarization (fADP) were also assessed using a minimal-activity protocol. In this protocol, single action potentials were elicited no more than 10 times every 5 min for up to 1 h. These action potentials were elicited using a brief (2 ms) current step, the amplitude of which was set to be within 20 pA of the threshold current ($I_{threshold}$). Determination of $I_{threshold}$ required varying the current

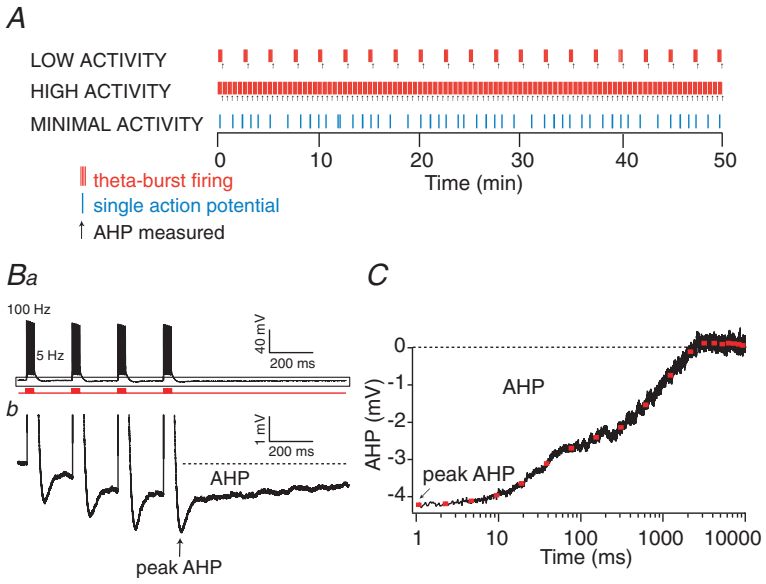

Figure 1. The afterhyperpolarization (AHP) triggered with theta-burst firing
A, schematic diagram of current injections for the low, high and minimal activity conditions. Upward arrow denotes where the AHP occurs. *Ba*, typical example theta-burst firing in response to brief suprathreshold depolarizing current steps (1nA for 2 ms) delivered via a somatic whole-cell recording electrode ($I_{electrode}$, red) in a CA1 pyramidal neuron. *Bb*, shows membrane potential (noted in black rectangle above), including the AHP, on an expanded scale. *C*, plot of AHP *versus* time on a log scale (black). Area under the dotted line represents the AHP integral. The AHP was averaged into bins (red squares, see Methods).

amplitude over the course of the recording; therefore, the time interval between spikes with minimal activity was variable over the duration of the recording and across cells. An example from one neuron is shown in Fig. 1*A*.

Finally, in order to examine AHP plasticity, a high-activity protocol was delivered to neurons in whole-cell configuration using either KMeth or KGluc (Fig. 1*A*). The only differences between the low- (previously described) and high-activity groups was the frequency at which we repeatedly elicited the AHP (Fig. 1*A*, arrows) and the total number of action potentials. For the high-activity protocol, an AHP was elicited using theta-burst firing once every 30 s, resulting in a total of 200 action potentials per 5 min, for up to 1 h.

In all experiments, initial measurements of the R_N were performed directly following compensation for capacitance and series resistance, approximately 30–60 s after gaining access to the neuron; this point corresponds to the value at 0 min on all graphs. Values determined within the first 2.5 min are referred to as 'immediate'. R_N was monitored at least once per minute for the duration of the recordings.

Data acquisition and analysis

Data were transferred to a computer using an ITC-16 analog-to-digital converter (InstruTech, Port Washington, NY, USA). Igor Pro (Wavemetrics, Lake Oswego, OR, USA) and pCLAMP (Axon Instruments, Sunnyvale, CA, USA) software were used for acquisition and analysis. Statistical tests were performed using SPSS software (SPSS Inc., Chicago, IL, USA). Significance was determined by repeated measures ANOVA or one-way ANOVA with *post hoc* Fisher's least significant difference *t* tests where appropriate (unless otherwise noted). All results are reported as means ± S.E.M.

The AHP was defined as the membrane potential beginning at the peak negative value relative to the initial baseline (Fig. 1*B*, dashed line) following the last spike (Fig. 1*Bb*, arrow) and ending when the voltage had decayed to 95% of that peak value. The integral of the AHP was calculated and shown in Fig. 1*C* as the area under the dashed line. The AHP was then divided into bins of varying durations (Fig. 1*C*, red squares). In order to facilitate repeated-measures statistical comparisons of AHPs obtained under different conditions, the fast repolarizing component of the AHP (the first 1000 ms) was divided into bins of varying duration (y, in milliseconds), according to the equation $y = i \times 2^{(x+1)}$, where i is the sample interval (0.05 ms for 20 Hz sampling rate), $2^{(x+1)}$ is the number of points being averaged, and x is the bin number (beginning with $x = 0$). The value of the AHP (in millivolts) was determined by the average V_m in each bin and plotted against time on a log scale beginning at 1 ms after the AHP peak (Fig. 1*C*). Each point is plotted at a time equal to the mid-point of the bin. This approach afforded us the ability to sample the early component of the AHP at a very high rate, while gradually reducing the sampling rate as the magnitude of the AHP decreased over time. Because the AHP slowly decays after 1 s, the remainder of the AHP (> 1000 ms) values were averaged into bins of 1024 ms. AHPs were compared among groups by applying repeated measures ANOVA on the log-sampled points.

The medium AHP (mAHP) and the slow AHP (sAHP) were identified by their differential sensitivity to the bee venom apamin (100 nM) and noradrenaline (10 μM). For ease of comparisons, the average membrane potential at 1 ms corresponds to the peak of the apamin-sensitive AHP (mAHP) and the average membrane potential at 1 s corresponds to the apamin-insensitive AHP (sAHP) (for review see Storm, 1990; Stocker *et al.* 1999).

The fADP was measured following a single action potential. The fADP amplitude was reported as the average membrane potential, relative to the resting membrane potential, in the first 10 ms after the fast repolarization phase of the action potential, as previously described (Metz *et al.* 2005). The total fADP was reported as the integral of the fADP beginning after the fast repolarization phase of the action potential and terminating when membrane potential returned to the resting value. Action potential threshold was defined as the voltage (V) when dV/dt first exceeded 28 mV ms^{-1} and was confirmed by eye as corresponding to the inflection point at which the action potential began. The action potential amplitude (spike height) was defined as the change in voltage from action potential threshold to the maximum voltage achieved during the action potential, as previously described (Golding *et al.* 2001). $I_{threshold}$ was defined as the amount of current required to trigger one action potential and determined by incrementally increasing the amplitude of a brief (2 ms) current step in 20 pA increments. The sag ratio was reported as the ratio of the steady-state voltage (average voltage during the last 100 ms), to the peak voltage (measured within the first 100 ms) in response to an 800 ms hyperpolarizing current step of −50 pA. R_N was determined by Ohm's law from the response to the same 800 ms, −50 pA current step. Membrane potentials were not corrected for the liquid junction potential, which was estimated to be −8 mV.

Results

Whole-cell and perforated patch-clamp recordings were obtained from 113 CA1 pyramidal neurons in rat hippocampal slices. Neurons had an average resting membrane potential of -60 ± 0.5 mV and an input resistance of 83 ± 4.0 MΩ (see Table 1). All cells

Table 1. Effects of the anion measured directly after membrane rupture (0 min)

	V_m (mV)	R_N (MΩ)	R_S (MΩ)	Threshold (mV)	$I_{threshold}$ (pA)	Spike height (mV)	Sag ratio (SS/peak)
KMeth (49)	−60 ± 1	84 ± 8	17 ± 3	−54 ± 1	1048 ± 168	95 ± 4	0.82 ± 0.02
KGluc (34)	−60 ± 1	72 ± 7	16 ± 3	−53 ± 1	1249 ± 144	103 ± 2†	0.76 ± 0.02†
Perforated (9)	−63 ± 0.3*†	89 ± 9*	31 ± 6*†	−49 ± 2 *†	1135 ± 106	88 ± 6*†	0.70 ± 0.03*†

Number of cells per group are indicated in parentheses. One-way ANOVA with *post hoc* LSD *t* test, *$P < 0.05$ compared to KGluc; †$P < 0.05$ compared to KMeth.

demonstrated a prominent AHP (a negative membrane potential relative to baseline) following a train of action potentials (Fig. 1).

Effects of the main internal anion on the apamin-sensitive AHP

In order to determine the effects of the internal anion on the two major components of the AHP, the mAHP and sAHP components, we first segregated the AHPs based on their sensitivity to the bee venom apamin (100 nM). Application of apamin, a selective small-conductance calcium-activated potassium channel blocker of type 2 and 3 (SK2 and SK3), reduced the average membrane potential of the AHP for no longer than 1 s; apamin had no effect on the AHP lasting > 1 s (Fig. 2). Therefore, we refer to the portion of the AHP that is sensitive to apamin as the mAHP (1 ms to 1 s).

An apamin-sensitive mAHP was observed in recordings using KMeth and KGluc ($n = 3$ per group, Fig. 2*A*–*C*). Although the relative amplitude of the apamin-insensitive mAHP was significantly reduced in KGluc (49 ± 5% of baseline) compared to in KMeth (79 ± 9%, $P < 0.05$), the absolute amplitude of the apamin-sensitive mAHP was similar in KGluc and KMeth (−0.85 ± 0.05 and −1.55 ± 0.65 mV, respectively, $P = 0.4$). Apamin has been shown to selectively block the AHP current (I_{AHP}) (Kohler *et al.* 1996; Stocker *et al.* 1999), and therefore these data suggest that the I_{AHP} size does not depend on the internal anions used in the present study.

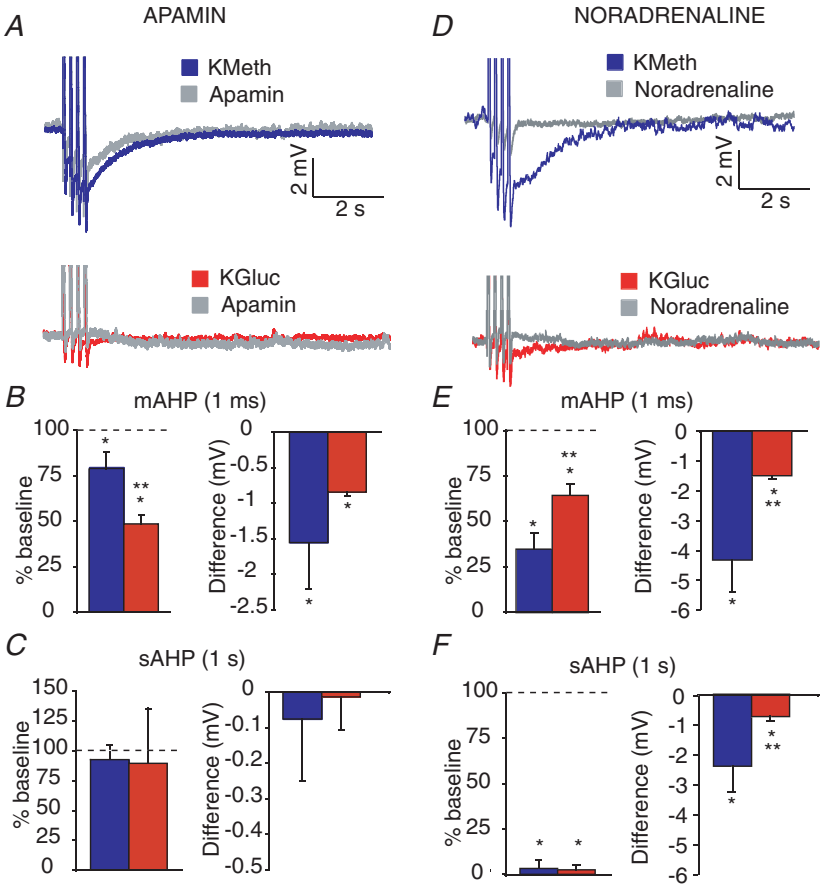

Figure 2. Whole-cell recordings showing distinct apamin-sensitive and noradrenaline-sensitive AHPs
A, apamin sensitivity of AHPs recorded with KMeth (blue) and KGluc (red). Representative example of the AHPs before (blue or red) and after (grey) bath application of apamin (100 nM). *B*, the mAHP (apamin sensitive) was significantly reduced in the presence of apamin (*$P < 0.05$ compared to baseline). The percentage reduction by apamin normalized to the baseline mAHP was significantly greater in KGluc than in KMeth (**$P < 0.05$). But the mean difference in voltage of the mAHP following subtraction was not different between KMeth and KGluc. *C*, no effect of apamin was observed during the sAHP (apamin insensitive) measured at 1 s. *D*, noradrenaline sensitivity of AHPs recorded with KMeth (blue) and KGluc (red). Representative example of the AHPs before (blue or red) and after (grey) bath application of noradrenaline (10 μM). *E*, the remainder of the mAHP (the apamin-insensitive component) was significantly reduced in the presence of noradrenaline (*$P < 0.05$ compared to baseline). The percentage reduction by noradrenaline normalized to the baseline mAHP was significantly greater in KMeth than in KGluc (**$P < 0.05$) and the mean difference in voltage of the mAHP following subtraction was larger in KMeth than in KGluc (**$P < 0.05$). *F*, the sAHP was significantly reduced by noradrenaline measured at 1 s.

Effects of the main internal anion on the noradrenaline-sensitive component of the mAHP

As apamin only partially blocked the mAHP, we hypothesized that the remainder of the mAHP may be driven by the activation of the slow AHP current (sI_{AHP}), as suggested previously by Stocker *et al.* (1999). We examined the contribution of the sI_{AHP} to the mAHP (1 ms to 1 s) via bath application of noradrenaline (NA), a neuromodulator shown to selectively reduce the sI_{AHP} without significantly altering currents ascribed to the mAHP, specifically the I_{AHP} (Sah, 1996; Shah & Haylett, 2000) and M-current (I_M) (Madison & Nicoll, 1986; Storm, 1989). In line with this hypothesis, bath application of NA significantly reduced the mAHP ($n = 3$ per group, Fig. 2*D–F*). A greater fraction of the mAHP was inhibited by NA in recordings using KMeth compared to those using KGluc (reduced to $34 \pm 8\%$ and $63 \pm 6\%$ of baseline, respectively, $P < 0.05$). Moreover, the absolute amplitude of the NA-sensitive mAHP was significantly greater in recordings using KMeth than in those using KGluc (-4.3 ± 1 and -1.5 ± 0.1 mV, respectively, $P < 0.05$). These data support the contention that the sI_{AHP} also contributes to the mAHP that directly follows a train of action potentials and that this current is larger in recordings using KMeth than in those using KGluc.

Effects of main internal anion on the NA-sensitive component of the sAHP

In line with previous reports, we observed no effect of apamin on the AHP measured at 1 s or later in recordings using either KMeth or KGluc (reduced to $93 \pm 12\%$ and $90 \pm 46\%$ of baseline, respectively). The apamin-insensitive AHP measured at 1 s post burst is generally referred to as the sAHP and is thought to be mediated by the Ca^{2+}-dependent sI_{AHP}. In support of this, 10 μM NA blocked the sAHP in recordings performed using KMeth or KGluc (reduced to $3 \pm 4\%$ and $2 \pm 2\%$ of baseline, respectively), which is consistent with previous reports (Haas & Konnerth, 1983; Madison & Nicoll, 1986; Costa *et al.* 1992; Sah, 1996). Although the relative amplitude of the NA-sensitive component of the sAHP was similar in recordings using KMeth or KGluc, the absolute amplitude of the NA-sensitive sAHP was larger in KMeth than in KGluc (-2.4 ± 0.9 and -0.75 ± 0.1 mV, respectively, $P < 0.05$).

Next, we set out to examine whether the action of NA was specific to blockade of a Ca^{2+}-dependent K^+ current (Madison & Nicoll, 1984, 1986), as opposed to inhibition of the Na^+-mediated K^+ current shown to underlie a late AHP in neocortical neurons (Foehring *et al.* 1989). This distinction is important given recent evidence that Na^+-activated K^+ channels (Slo2) believed to underlie the late-AHP in neocortical cells are also expressed in the hippocampus (Bhattacharjee *et al.* 2002; for review see Bhattacharjee & Kaczmarek, 2005) and share common modulator pathways (Santi *et al.* 2006). Therefore, we tested the effects of the divalent calcium channel blocker Cd^{2+} (200 μM) on the mAHP (1 ms) and sAHP (1 s). Cd^{2+} significantly reduced the mAHP and sAHP to levels achieved by NA alone in recordings with KMeth (reduced to $35 \pm 5\%$ and $4 \pm 22\%$ of baseline, respectively, $n = 4$) and KGluc (reduced to $55 \pm 8\%$ and $2 \pm 14\%$ of baseline, respectively, $n = 4$) (Fig. 1 in Supplemental material). Taken together, these data confirm that the effects of NA on the mAHP and sAHP are mediated by a reduction in the Ca^{2+}-dependent sI_{AHP}.

Comparisons of the AHP using whole-cell and perforated-patch recordings

Because the AHP was larger in KMeth than in KGluc, we were interested in determining whether KMeth artificially enhances the AHP or whether KGluc artificially reduces it. We hypothesized that immediate measurements of the AHP performed prior to dialysis of the neuron with internal solution would be similar in KMeth and KGluc, and thus reflect the AHP under more physiological conditions.

We tested the immediate effects of the internal anion on the AHP and membrane properties, prior to complete dialysis, in 30 neurons using whole-cell recordings with either KMeth ($n = 21$) or KGluc ($n = 9$). AHPs elicited from theta-burst firing and 50 Hz firing were measured immediately (within 2.5 min) after obtaining a whole-cell recording. Contrary to our hypothesis, the average negative membrane potential, relative to baseline, during the mAHP (1 ms) and sAHP (1 s), was significantly greater in KMeth than in KGluc ($P < 0.05$; Fig. 3 and Table 2). These data suggest that the effects of the internal anion alter the AHP within about 2 min of establishing the whole-cell configuration.

Because even the immediate measures of the AHP and membrane properties were confounded by the internal solution in whole-cell recordings, we performed perforated-patch recordings to determine which internal solution best emulates cellular physiology under more natural conditions (i.e. without dialysis of the internal solution). We compared the mean amplitude of AHPs of CA1 pyramidal neurons in perforated-patch ($n = 9$) and whole-cell recordings using either KMeth ($n = 21$) or KGluc ($n = 9$).

As predicted by previous experiments using sharp microelectrode recordings (Zhang *et al.* 1994), the mean amplitude of the mAHP measured in perforated-patch recordings was closer to that measured using KMeth in whole-cell recordings (Fig. 3). This result was true for an mAHP triggered by either a 50 Hz train

Table 2. Effects of internal anion on the AHP: comparison with perforated-patch recording

	50 Hz		Theta	
	mAHP (mV)	sAHP (mV)	mAHP (mV)	sAHP (mV)
KMeth (21)	-5.6 ± 0.4*	-2.3 ± 0.3*	-5.8 ± 0.5*	-2.9 ± 0.4*
KGluc (9)	-3.7 ± 0.6#	-1.2 ± 0.3†	-3.7 ± 0.5†	-1.7 ± 0.3†
Perforated (9)	-6.7 ± 0.7*†	-2.0 ± 0.4*	-5.2 ± 0.5*	-1.9 ± 0.3†

Number of cells per group are indicated in parentheses. One-way ANOVA with *post hoc* LSD *t* test, *$P < 0.05$ compared to KGluc; †$P < 0.05$ compared to KMeth.

or theta-burst firing. The mean amplitude of the mAHP in perforated-patch recordings was not different (perforated ≈ KMeth with theta-burst firing, $P = 0.6$) or was significantly increased (perforated > KMeth with 50 Hz train, $P < 0.05$) compared to whole-cell recordings with KMeth. The mAHP was significantly smaller in whole-cell recordings made using KGluc compared to both perforated-patch and KMeth ($P < 0.05$). Therefore, whole-cell recordings using KMeth best emulate the mAHP observed in the more natural conditions of perforated-patch recordings.

Similarly, the sAHP elicited using a 50 Hz train (50 Hz–sAHP) in whole-cell recordings using KMeth was more similar to perforated-patch recordings (see Table 2). The 50 Hz–sAHP in KGluc was significantly smaller than the sAHP in both KMeth and perforated-patch recordings ($P < 0.05$). These data replicated earlier reports that showed that the AHP is inhibited by KGluc (Zhang *et al.* 1994; Velumian *et al.* 1997). Based on the results of our statistical analysis, the 50 Hz–sAHP measured in perforated-patch recordings was not different from whole-cell recordings using KMeth ($P = 0.4$). Visual

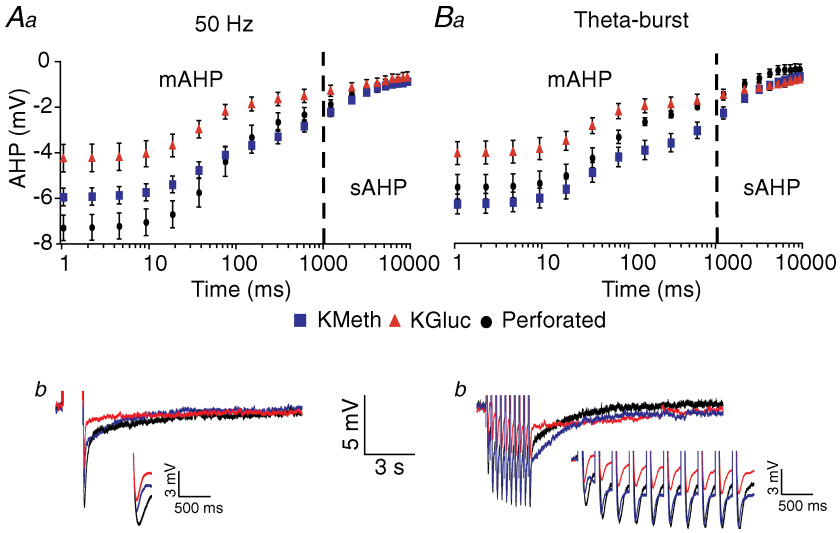

Figure 3. The main anion has an immediate effect on the AHP, and perforated-patch recordings show that mAHPs and the early 50 Hz–sAHP, but not early theta–sAHP, are best emulated in KMeth
A, AHP evoked by 50 Hz train of action potentials. *B*, AHP evoked by theta-burst firing. *Aa*, summary graph illustrates the average membrane potential of the binned 50 Hz–AHP measured immediately after obtaining a whole-cell recording using KMeth (blue) or KGluc (red), or after gaining access in perforated-patch configuration (black). *Ab*, shows typical 50 Hz–sAHPs (triggered with 50 action potentials at a frequency of 50 Hz) in whole-cell recordings using KMeth or KGluc, or in perforated-patch configuration. Inset shows mAHP on an expanded scale. *Ba*, summary graph illustrates the average membrane potential of the binned theta-AHP measured in whole-cell recordings immediately after obtaining a whole-cell recording using KMeth or KGluc, or in perforated-patch configuration. *Bb*, shows typical theta–sAHPs (triggered with 10 bursts at 5 Hz where each burst consisted of five action potentials at 100 Hz) in whole-cell recordings using KMeth or KGluc, or in perforated-patch configuration. Inset shows mAHP on an expanded scale. The early sAHP (1 s) triggered by theta-burst firing was best emulated by recordings using KGluc when compared to perforated-patch recordings. The mAHP triggered with theta-burst firing was most similar in KMeth compared to perforated-patch recordings.

Table 3. Effects of the anion during minimal stimulation (10 min)

	R_s (MΩ)	R_N (MΩ)	Threshold (mV)	$I_{threshold}$ (pA)	Spike height (mV)
KMeth (10)	18 ± 4	85.7 ± 8.6*	−54.3 ± 1*	907 ± 152*	96 ± 4
KGluc (10)	18 ± 2	61.7 ± 10.1	−51.9 ± 1	1257 ± 139	101 ± 3

Number of cells per group are indicated in parentheses. One-way ANOVA with *post hoc* LSD *t* test, $^*P < 0.05$ compared to KGluc.

inspection of the results (Fig. 3*A*) indicated that although the 50 Hz–sAHP in perforated configuration was not statistically different from that in KMeth, the average 50 Hz–sAHP measured with perforated-patch falls in between those measured in KMeth and KGluc. As expected, the AHP in perforated-patch recordings was not affected by the internal anion (KMeth and KGluc; $P = 0.4$), because these anions are too large to pass through the perforations in the membrane. These data confirm and refine earlier reports demonstrating the inhibitory effects of KGluc on AHPs elicited with conventional high-frequency (50 Hz) stimulation protocols.

Surprisingly that the sAHP triggered with theta-burst firing (theta–sAHP) using perforated-patch recordings was more similar to that measured in whole-cell recordings using KGluc rather than KMeth (KMeth, −2.9 mV ± 0.4; KGluc, −1.7 ± 0.3 mV; perforated, −1.9 ± 0.3 mV). The theta–sAHP in KMeth was significantly increased compared to both KGluc and perforated-patch recordings (KGluc *versus* perforated, $P = 0.8$; KMeth *versus* KGluc, $P < 0.05$; KMeth *versus* perforated, $P < 0.05$). Therefore, it appears that under some circumstances, KMeth may artificially enhance the AHP (Fig. 3*B*). Because each cell was stimulated with both 50 Hz and theta-burst firing patterns in an alternating fashion, the restricted enhancement of the theta–sAHP in KMeth suggests that the underlying currents may be different between AHPs triggered with theta-burst firing and a 50 Hz train. These data are summarized in Table 2.

Immediate effects of main internal anion on other membrane properties

Differential effects of the main anion on other membrane properties were also observed directly after obtaining whole-cell recordings (Table 1). One of the most notable differences was the size of the action potential and the fADP that follows it in CA1 pyramidal neurons. Both the action potential and the fADP (Fig. 4) were smaller in KMeth than in KGluc ($P < 0.05$). In addition, the sag ratio was significantly increased in KMeth compared to KGluc ($P < 0.05$). Although no significant differences in V_m, R_N, R_s, threshold and $I_{threshold}$ were observed between the two internal solutions immediately following membrane rupture in whole-cell recordings (Table 1), R_N, threshold and $I_{threshold}$ were significantly different after further dialysis (5–10 min) in KMeth compared to KGluc (Table 3).

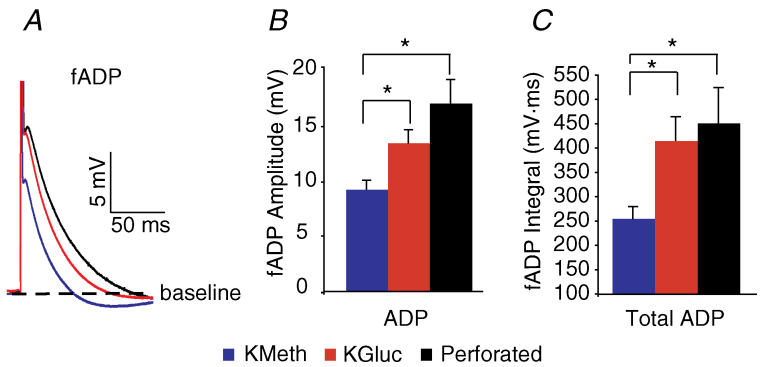

Figure 4. The fast afterdepolarization (fADP) in KGluc best emulates perforated-patch recordings
A, typical examples of the fADP superimposed at early time points in whole-cell recordings using KMeth (blue) or KGluc (red) and in perforated-path configuration (black). The integral of the fADP is calculated up to the time V_m crosses the baseline potential. *B*, bar chart of the average amplitude of the fADP measured immediately after obtaining a whole-cell recording using KMeth (blue) or KGluc (red) or in perforated-patch configuration (black). The amplitude of the fADP measured at the early time point was significantly reduced using KMeth compared to using KGluc and perforated-patch recordings ($^*P < 0.05$). *C*, bar chart of the average integral of the fADP measured immediately after obtaining a whole-cell recording using KMeth or KGluc or in perforated-patch configuration. The integral of the fADP measured at the early time point was significantly reduced using KMeth compared to ussing KGluc and perforated-patch recordings ($^*P < 0.05$).

Comparisons of membrane properties using perforated-patch recordings

Using perforated-patch recordings, we determined that the amplitude and integral of the fADP is best preserved in whole-cell recordings using KGluc (amplitude, $P = 0.1$; integral, $P = 0.7$). The amplitude and integral of the fADP in KMeth were significantly reduced compared to the values in KGluc and perforated-patch recordings (Fig. 4; $P < 0.05$).

Furthermore, the sag ratio was lowest in perforated-patch recordings (Table 1), indicative of more hyperpolarization-activated cation current active at rest, compared to whole-cell recordings with both KMeth and KGluc ($P < 0.05$). This result suggests there may be some rundown of the hyperpolarization-activated cation current in whole-cell recordings. We also observed a higher action potential threshold in perforated-patch compared to whole-cell recordings, which additionally resulted in a reduction in spike height (measured from threshold to the peak of the action potential, $P < 0.05$). Finally, R_N and R_S in perforated-patch recordings were significantly higher than in whole-cell recordings ($P < 0.05$). These data are summarized in Table 1. Again, these data show that the internal anion can significantly alter the AHP and membrane properties within tens of seconds after rupture.

Gradual effects of the main internal anion on the AHP

We next tested the gradual effects of KMeth- and KGluc-based internal solution on the AHP and basic membrane properties in whole-cell recordings. We evoked the AHP using theta-burst firing at a low rate (once every 150 s; low activity) in order to minimize activity-dependent changes in neuronal excitability (Borde *et al.* 1995).

Previous studies suggested that internal perfusion of KMeth preserves the ionic currents underlying the AHP. Therefore, we hypothesized that the AHPs would be comparable in size and stability over a long whole-cell recording using KMeth. Indeed, we observed that the mean amplitude of the mAHP and sAHP measured in whole-cell recordings using KMeth ($n = 8$) were stable over the duration of the experiment in the low-activity group (Fig. 5*A* and *C*, $P = 0.8$).

Because previous reports demonstrated that internal perfusion of KGluc produces a rundown of the respective currents that underlie the mAHP and sAHP (Zhang *et al.* 1994; Velumian *et al.* 1997), we expected that the AHP measured in KGluc would decrease progressively over time. Contrary to this expectation, however, the AHPs evoked under conditions of low-activity were remarkably stable in KGluc (Fig. 5*B* and *D*); the mAHP and sAHP were comparable throughout the experiment. Repeated measures ANOVA revealed no significant effect of time on the amplitude of the AHP in the low-activity condition ($n = 4$, $P = 0.8$).

Gradual effects of the main internal anion on the fADP

Because the fADP is an important determinant of neuronal output, we examined the effects of the internal anion on the amplitude of the fADP over time. To do this, we triggered single spikes and measured the fADP at the early (0–10 min) and late (35–45 min) time points in low-activity conditions. All cells responded to a brief current injection with a single action potential. The fADP measured using KMeth at the late time point was markedly reduced ($P < 0.05$); in contrast, the fADP in KGluc was stable (Fig. 6*A*). These data suggest that the fADP undergoes a passive rundown in whole-cell recordings using KMeth, but not KGluc.

In order to directly test the hypothesis that the fADP is altered as a consequence of KMeth, regardless of any theta-burst firing, we repeated the above experiment using a minimal-activity protocol ($n = 10$ per group). Under these conditions, theta-burst firing was omitted and no more that five to 10 single spikes were elicited every 5 min (Fig. 1*A*). As in the low-activity experiments, a significant reduction of the fADP occurred with KMeth, even under minimal-activity conditions ($P < 0.05$). Thus, the effect on the fADP is time dependent, but not activity dependent. The stability of the fADP in KGluc compared to in KMeth is illustrated in Fig. 6*B* and *C*. These data suggest that the firing mode and excitability of CA1 pyramidal neurons is significantly altered in whole-cell recordings using KMeth, especially at later time points.

Gradual effects of the main internal anion on R_N

Neuronal excitability can also be influenced by changes in the basic membrane properties of the cell. In whole-cell recordings using KMeth, we observed a gradual increase in R_N and a gradual reduction of the $I_{threshold}$ (Fig. 7). Conversely, R_N and $I_{threshold}$ were stable in whole-cell recordings in KGluc. R_N was significantly increased (165% of control, $P < 0.05$) after 50 min of recording under conditions of low-activity using KMeth compared to using KGluc (93% of control). The effect of KMeth on R_N was independent of any activity-related alterations in intrinsic excitability because no significant differences in the KMeth-induced increase in R_N were observed in conditions of low or minimal activity (KMeth, $164 \pm 4\%$, $P = 0.4$). This significant time-dependent increase in R_N observed using KMeth (repeated measures ANOVA, $P < 0.05$) was not observed in recordings with KGluc. This result was observed in neurons from young (14–28 days)

and mature rats (35–55 days). A one-way ANOVA with *post hoc* least-significant difference (LSD) *t* tests revealed no significant difference in R_N across age ($P = 0.3$), and no significant interaction between age and internal solution ($P = 0.9$). Measurements of R_N were therefore pooled from all cells for each internal solution, KMeth and KGluc, and plotted in Fig. 7*B* and *C* (high-activity data included, see below). Repeated measures ANOVA revealed ($P = 0.6$)

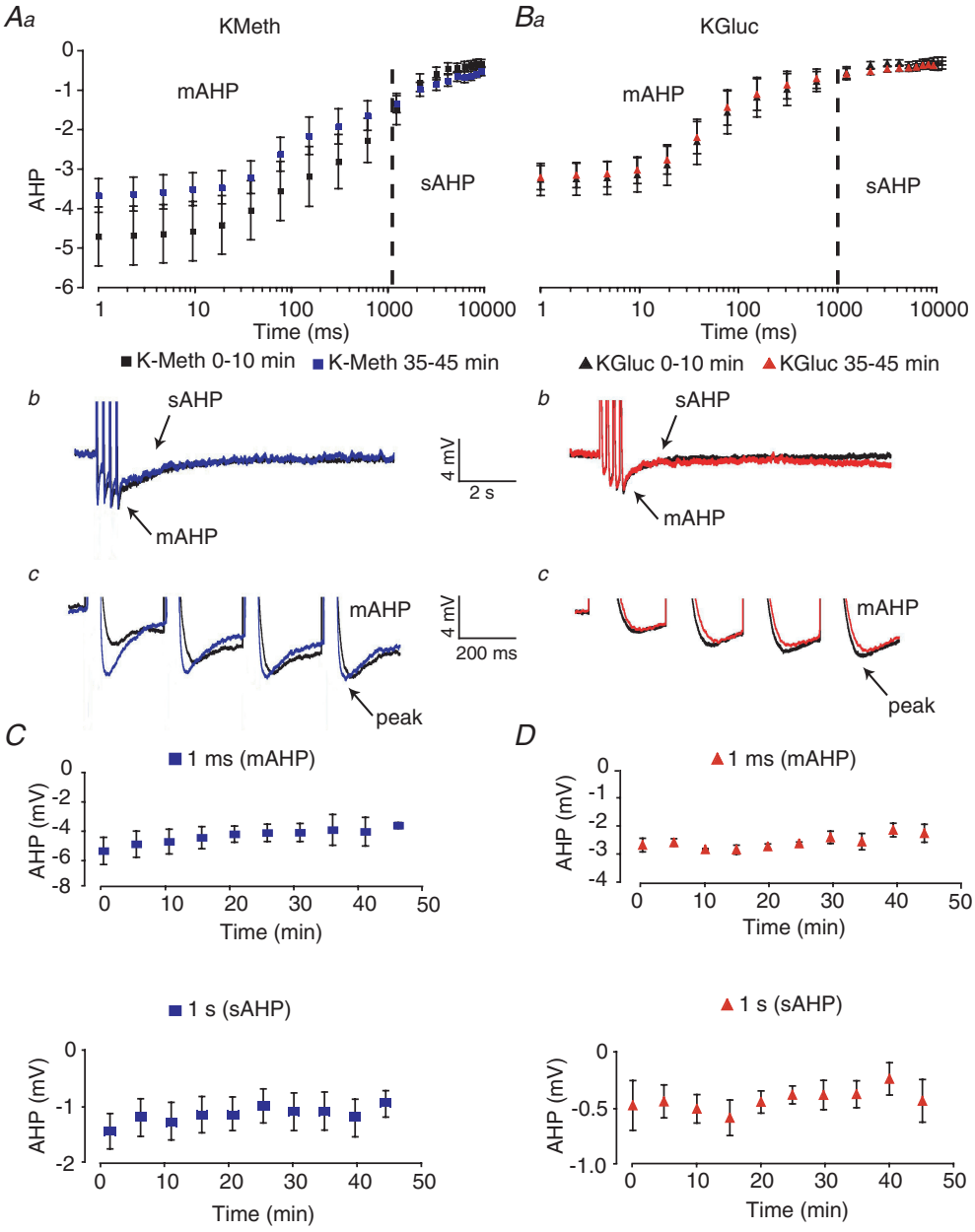

Figure 5. Stability of the AHP in whole-cell recordings using theta-burst firing in a low-activity protocol
A, repeated theta-burst firing at a low rate (once every 150 s) did not alter excitability of CA1 pyramidal neurons in whole-cell recordings using KMeth. *Aa*, summary graph illustrates the stability of the average membrane potential of the binned AHP at the early (0–10 min) and late (35–45 min) time points. *Ab*, representative trace of the AHP triggered at the early (black) time point superimposed on the AHP triggered at the late (blue) time point. *Ac*, the mAHP displayed in *Ab* on an expanded time scale. *B*, repeated theta-burst firing at a low rate (once every 150 s) did not alter excitability of CA1 pyramidal neurons in whole-cell recordings using KGluc. *Ba*, summary graph illustrates the stability of the average membrane potential of the binned AHP at the early (0–10 min) and late (35–45 min) time points. *Bb*, representative trace of the AHP triggered at the early (black) time point superimposed on the AHP triggered at the late (red) time point. *Bc*, the mAHP displayed in *Bb* on an expanded time scale. *C*, plot of mean mAHP (1 ms) and early sAHP (1 s) with time in KMeth. *D*, plot of mean mAHP (1 ms) and early sAHP (1 s) with time in KGluc. For all traces, the membrane potential of the neuron was held constant at −66 mV for the duration of the experiment by manually adjusting the holding current.

that R_S of neurons in KMeth was not statistically different from values of those in KGluc over the duration of the recordings. Importantly, preliminary results from our laboratory suggest that the effects of KMeth on R_N may not generalize to CA1 neurons of the mouse, which have a higher R_N compared to rat CA1 neurons (mouse, 161 ± 25 MΩ, $n = 6$, see Fig. 1 of Supplemental material; rat, 84 ± 8 MΩ, see Fig. 7) and remain stable over time using KMeth. The high R_N of the mouse CA1 pyramidal neurons may reflect merely a size difference between CA1 neurons from rat and mouse and/or differences in the contribution of ionic conductances active at the resting membrane potential.

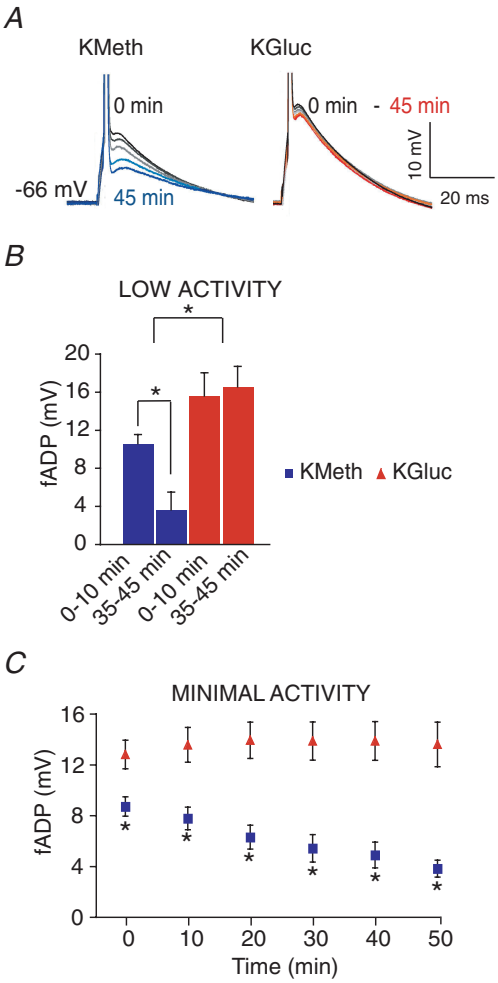

Figure 6. The fast afterdepolarization (fADP) is smaller and exhibits rundown in whole-cell recordings using KMeth, but is stable using KGluc
A, typical examples of the fADP from multiple time points in whole-cell recordings using KMeth (blue) or KGluc (red). *B*, bar chart of the average amplitude of the fADP measured using either KMeth (blue) or KGluc (red) at the early (0–10 min) and late (35–45 min) time points with the low-activity protocol. The amplitude of the fADP measured at the early time point was significantly reduced when using KMeth compared to using KGluc (*$P < 0.05$). *C*, time course and magnitude of the fADP reduction with KMeth using the minimal-activity protocol. Repeated measures ANOVA revealed that whole-cell recording using KMeth resulted in both an immediate and time-dependent reduction of the fADP (*$P < 0.05$) compared to recordings using KGluc.

Plasticity of the AHP depends on the main internal anion

Finally, we tested the effects of KMeth and KGluc on the activity-dependent plasticity of the AHP of CA1 pyramidal neurons. Here we assessed the AHP over time in response

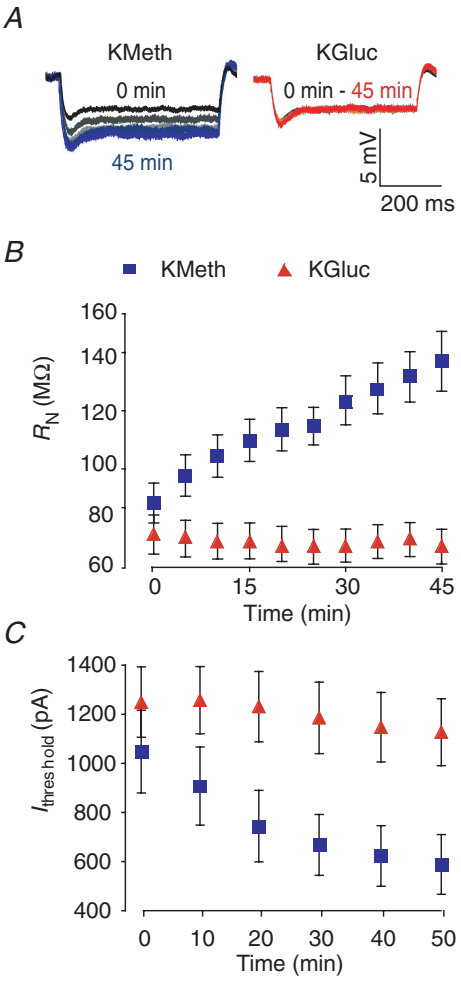

Figure 7. KMeth increases neuronal excitability and input resistance (R_N)
A, superimposed responses to an 800 ms current injection (−50 pA) over 45 min in a representative whole-cell recording using KMeth (blue) compared to a whole-cell recording using KGluc (red). *B*, time course and magnitude of enhancement of the R_N produced in whole-cell recordings using KMeth (blue) compared to whole-cell recording using KGluc (red). *C*, shows a concomitant decrease in $I_{threshold}$ over time in recordings using KMeth but not using KGluc.

to theta-burst firing every 30 s (high activity); a rate of synaptic activity that has been previously demonstrated to alter neuronal excitability in CA1 hippocampal neurons (Borde *et al.* 1999).

AHPs evoked in the high-activity protocol ($n = 5$) were comparable over the duration of the whole-cell recordings using KMeth. Repeated measures ANOVA revealed no significant effect of time on the amplitude of the mAHP or sAHP for the high-activity group (high, $P = 0.4$). Therefore, increasing neuronal activity appeared to have no effect on any component of the AHP for the duration of whole-cell recordings made using KMeth (Fig. 8*A* and *C*).

In contrast, AHPs were markedly reduced over time in response to the high-activity protocol in whole-cell recordings with KGluc. The mean amplitude of the mAHP was significantly reduced over time under conditions of high activity, as revealed by repeated measures ANOVA (Fig. 8*B*, $n = 5$, $P < 0.05$). There were no significant differences in the sAHP measured in KGluc when we considered time points from 1 to 10 s ($P = 0.9$). However, the mAHP and sAHP measured at 1 ms and 1 s, respectively, were significantly reduced across the duration of the experiment (Fig. 8*D*, $P < 0.05$). Thus, the mAHP and early sAHP (1 s) were reduced in conditions of high activity, but not low activity, suggesting that the reduction was activity dependent, as opposed to a non-specific rundown (Zhang *et al.* 1994; Velumian *et al.* 1997). Because these recordings were obtained in the presence of synaptic blockers, the plasticity of the AHP observed here reflects a change in the intrinsic properties of the neuron.

Plasticity of the AHP is long term

To test whether theta-burst firing induced a short-term or long-term reduction in the AHP, we first induced plasticity using high-activity protocol for 20 min (Fig. 9, dark orange); this is an activity pattern that has been shown to induce AHP plasticity. After induction, we used the low-activity protocol as a series of AHP probe trials (Fig. 9, light orange). Because the low-activity protocol does not induce plasticity, any changes observed in the AHP during the probe trial indicate a change in the AHP that was maintained after the induction. Thus, we found that theta-burst firing (every 30 s) resulted in a long-term change in the AHPs (Fig. 9). Induction of AHP plasticity leads to significant decreases in both the mAHP and early sAHP, which were maintained for the duration of the probe trials ($P < 0.05$), in some cases up to 1 h post induction (data not shown).

Plasticity of the AHP is insensitive to apamin

Because the plasticity of the AHP was restricted to the mAHP and early sAHP, and synaptic activation has been shown previously to reduce the I_{AHP} (Sourdet *et al.* 2003), we hypothesized that the activity-dependent reduction of the AHP resulted mainly from a reduction in the apamin-sensitive AHP current (I_{AHP}). In order to test this hypothesis, the I_{AHP} was blocked using bath application of apamin (100 nM) for the duration of the high-activity protocol. Contrary to our hypothesis, induction of AHP plasticity was observed in the presence of apamin (Fig. 10). Both the mAHP and early sAHP were significantly reduced during the high-activity protocol under blockade of the I_{AHP} ($P < 0.05$). The magnitude and time course of AHP plasticity was unaltered in the presence of apamin compared to the high-activity protocol using KGluc ($P = 0.13$ and $P = 0.34$, respectively, repeated measures ANOVA). These data suggest that AHP plasticity is probably mediated by changes in the sI_{AHP} rather than the I_{AHP}.

High activity does not alter input resistance

Although we found that KMeth induced a time-dependent increase in R_N (Fig. 7), this effect was unaltered by increased postsynaptic firing, as there was no significant difference in the KMeth-induced increase in R_N under conditions of low, high or minimal activity (KMeth, $164 \pm 10\%$ of control), and no significant difference in the R_N in KGluc under the same conditions (KGluc, $100 \pm 4\%$, $P = 0.4$). Therefore measurements of R_N from cells exposed to low-, high- and minimal-activity protocols were pooled for comparisons between KMeth and KGluc (Fig. 7). Taken together, these data demonstrate that KMeth alters the R_N and excitability of CA1 neurons from rat over time regardless of activity level. However, R_N in KGluc is stable over time regardless of activity level.

Variations in R_N complicate interpretation of voltage-clamp recordings

Given that KMeth produces a steady increase in R_N, we hypothesized that plasticity of AHP currents induced by the high-activity protocol may be masked in current-clamp recordings. Therefore we examined the effects of the high-activity protocol on the AHP currents measured in the voltage-clamp configuration. Measurements of the AHP currents were first performed in voltage-clamp mode. Next, we switched to current-clamp mode to trigger plasticity using the high-activity protocol described above. Following induction, we returned to voltage-clamp mode and again measured the AHP currents. In line with our hypothesis, we observed a significant reduction in the currents underlying the AHP even though the AHP measured in current-clamp mode was unchanged (see Fig. 11*A* and *Bb*). However, the voltage-clamp recordings were significantly confounded by changes in R_N, as the

amplitude and time course of currents (including the Ca^{2+} spike) required to elicit Ca^{2+}-dependent K^+ currents were altered during the unclamped event (Fig. 11*Bc*). In fact, changes in R_N are highly correlated with reductions in the AHP currents. Although measurements of the actual I_{AHP} and sI_{AHP} may occur under conditions of reasonable voltage clamp (because the underlying currents are slow), the Ca^{2+} spike required for activation is not clamped

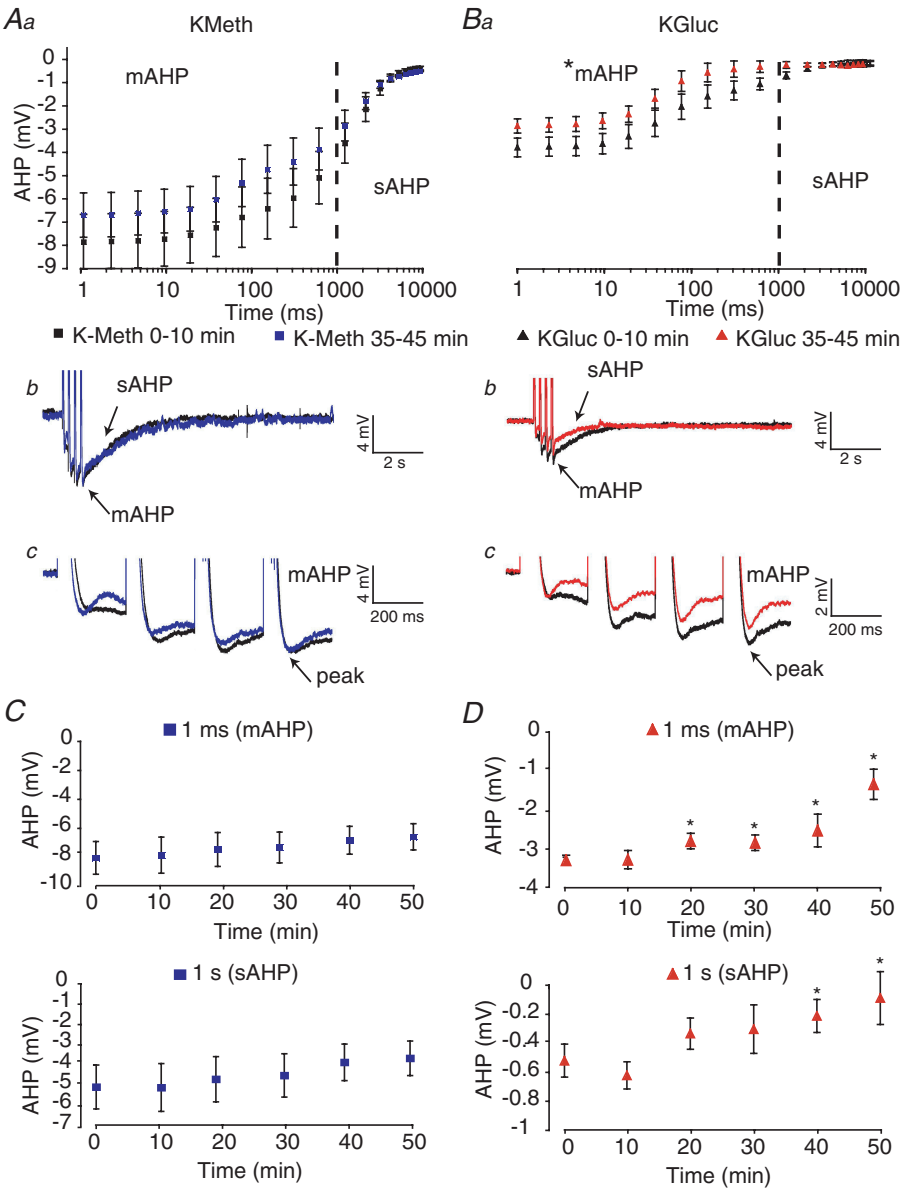

Figure 8. Repeated theta-burst firing induces an activity-dependent reduction in the AHP in whole-cell recordings using KGluc, but not KMeth

A, repeated theta-burst firing at a high rate (once every 30 s) did not alter excitability of CA1 pyramidal neurons in whole-cell recordings using KMeth. *Aa*, summary graph illustrates the stability of the average membrane potential of the binned AHP at the early (0–10 min) and late (35–45 min) time points. *Ab*, representative trace of the AHP triggered at the early time point (black) superimposed on the AHP triggered at the late time point (blue). *Ac*, the mAHP displayed in *Ab* on an expanded time scale. *B*, repeated theta-burst firing at a high rate (once every 30 s) induced a reduction in the AHP in whole-cell recordings using KGluc. *Ba*, summary graph illustrates the average membrane potential of the binned AHP at the late (35–45 min) time points was significantly reduced compared to the AHP measured at the early (0–10 min) time points. *Bb*, representative trace showing the AHP triggered at the early time point (black) superimposed on the AHP triggered at the late time point (red). *Bc*, the mAHP displayed in *Bb* on an expanded time scale. *C*, plot of mean mAHP (1 ms) and early sAHP (1 s) with time in KMeth. *D*, plot of mean mAHP (1 ms) and early sAHP (1 s) with time in KGluc. For all traces, the membrane potential of the neuron was held constant at −66 mV for the duration of the experiment by manually adjusting the holding current.

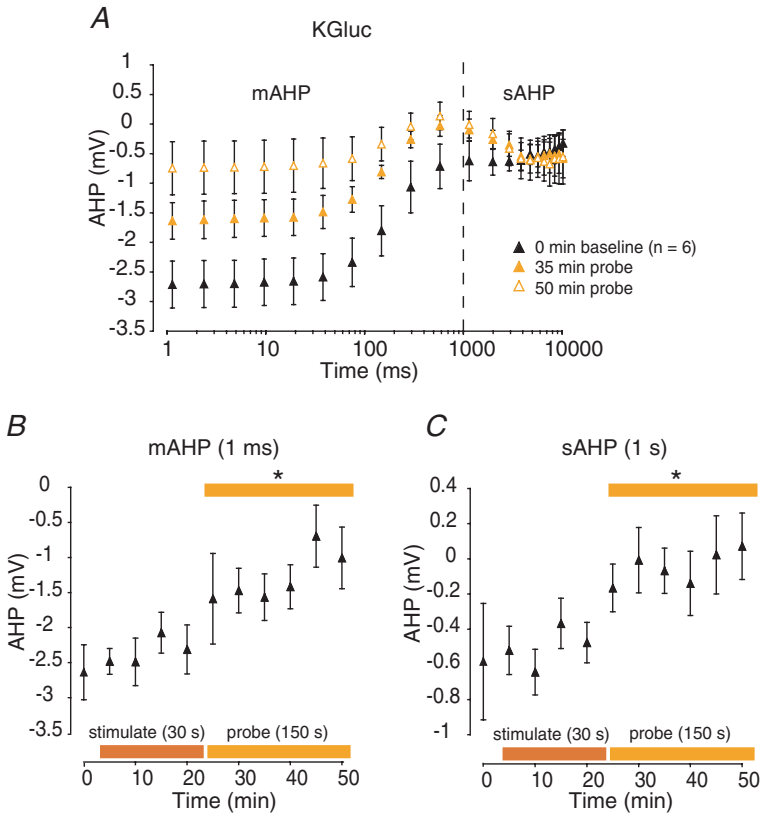

Figure 9. Long-term plasticity of the AHP in KGluc
A, summary graph illustrates the long-term reduction of the binned AHP measured during probe trials at 35 and 50 min time points (corresponding to 15 and 30 min post induction). *B*, the mAHP (1 ms) was significantly reduced during the probe trial period (25–50 min) as compared to the AHP measured at baseline (0 min). *C*, the sAHP (1 s) was significantly reduced during the probe trial period (25–50 min) as compared to the AHP measured at time 0 min (*$P < 0.05$ compared to baseline, repeated measures ANOVA).

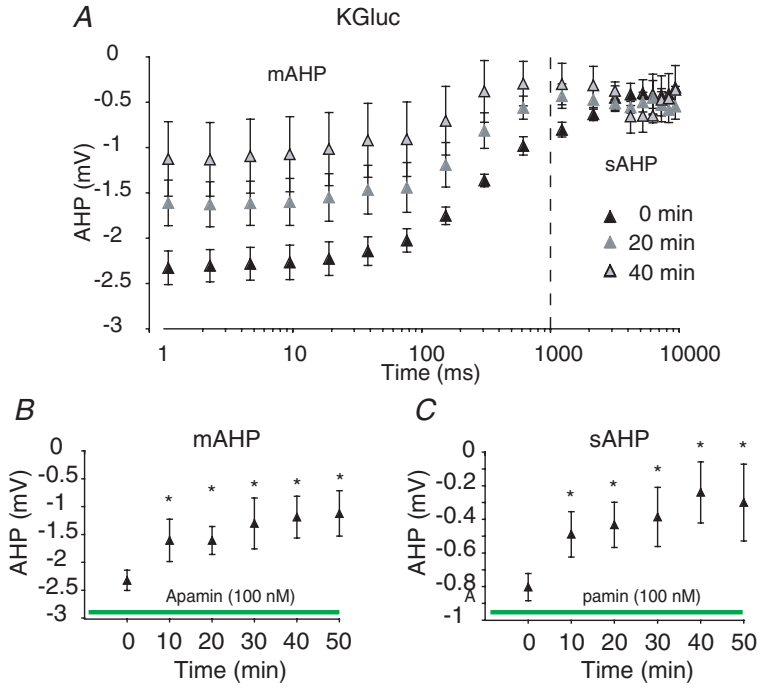

Figure 10. Plasticity of the apamin-insensitve AHP in KGluc
A, summary graph illustrates that the plasticity of the AHP during the high-activity protocol is preserved in the presence of apamin (100 nM). *B*, the mAHP (1 ms) was significantly reduced as compared to baseline (0 min). *C*, the sAHP (1 s) was significantly reduced as compared to baseline (0 min). Apamin was present prior to forming the seal or rupturing the membrane (shown in green), in order to insure maximal block prior to induction of plasticity. *$P < 0.05$ compared to baseline, repeated measures ANOVA.

well during the depolarizing voltage step, and is subject to variation as R_N changes. Therefore characterization of these currents is problematic, especially under conditions where R_N is variable.

Discussion

The results presented here have important implications for experiments requiring whole-cell recordings in CA1 pyramidal neurons from the rat. Our study demonstrates differences in the immediate and gradual effects of two widely used anions for whole-cell recordings – methylsulphate and gluconate – on membrane properties and plasticity. First, we show that immediate measures of the theta-burst-evoked sAHP are most accurate in KGluc, as determined by comparison with perforated-patch recordings. Second, KGluc produced stable measures of R_N and $I_{threshold}$ for up to 1 h, whereas R_N increased and $I_{threshold}$ decreased in KMeth. Third, induction of activity-dependent plasticity of the AHP was only observed in KGluc, whereas AHP plasticity was masked or blocked using KMeth. Fourth, activity-dependent changes in AHP were maintained for up to 1 h after induction. Taken together, these data suggest that KGluc provides a more stable long-term recording environment than KMeth.

One notable exception to the advantages of KGluc is that the mAHP and sAHP triggered by a 50 Hz train are smaller than those observed with KMeth or perforated-patch recordings. Therefore studies of the mAHP and sAHP triggered by a 50 Hz train require whole-cell recordings using KMeth. In some cases, perforated-patch recordings may be a better choice for long-term recordings where an increase in R_N is problematic, although these recordings have their own set of challenges (e.g. spontaneous rupture and high initial R_S that gradually decreases over time).

Effects of internal anion: new findings and comparison with previous reports

Our results regarding the effects of KMeth on R_N are consistent with some studies (Zhang *et al.* 1994; Robinson & Cameron, 2000), but appear inconsistent with a previous report that R_N increases when KMeth is replaced by KGluc (Velumian *et al.* 1997). The latter study is complicated, however, by the use of the anion replacement via pipette

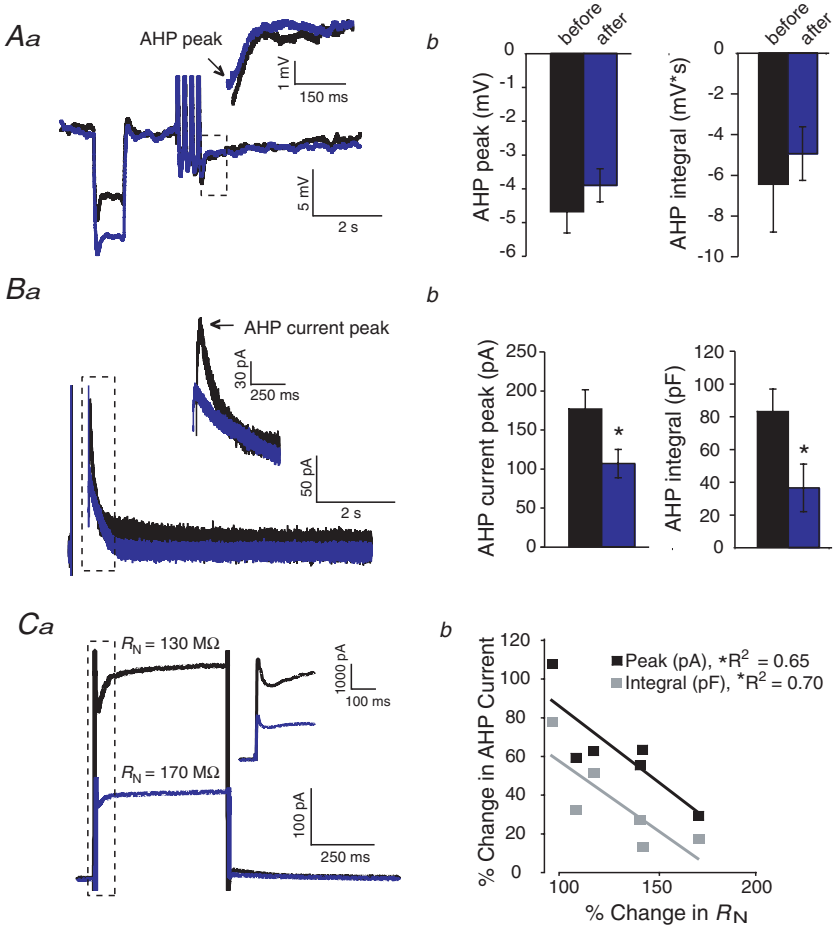

Figure 11. Changes in R_N differentially affect AHP and I_{AHP} in KMeth
Aa, representative traces demonstrating the stability of the AHP in KMeth after high-activity protocol (blue). *Ab*, The mean amplitude and integral of the AHP were not significantly different when measured before (black) and after (blue) exposure to the high-activity protocol. *Ba*, representative traces demonstrating the reduction of the AHP currents in KMeth after high-activity protocol (blue). *Bb*, A significant reduction in the peak and integral of the AHP currents when measured after (blue), compared to before (black), exposure to the high-activity protocol. *Ca*, representative traces where changes in the R_N may alter Ca^{2+} spike during the unclamped depolarizing step and confound measures of I_{AHP} and sI_{AHP}. *Cb* Plot of percentage change of the AHP currents by percentage change in R_N after exposure to high-activity protocol using KMeth. Changes in the R_N significantly correlate with changes in the peak and integral of the AHP measured in current-clamp mode. A negative relationship between the peak and integral of the AHP current, and R_N, is shown.

perfusion, as the exact time course and relationship between pipette perfusion and internal anion replacement are unclear. In fact, an earlier report from the same group, using standard whole-cell recordings (Zhang *et al.* 1994), is in better agreement with our results.

Both the present and previous reports (Zhang *et al.* 1994) demonstrate that the AHP is reduced in KGluc compared to in KMeth 5–10 min after obtaining a whole-cell recording. Furthermore, both studies show that KMeth best emulates AHPs elicited with a high-frequency train of action potentials when compared to either sharp-microelectrode or perforated-patch recordings. Based on the similarity of these reports, the novel findings demonstrated here concern the effects of the main anion on immediate measures of excitability of CA1 pyramidal neurons, long-term stability of membrane properties over time, AHPs evoked with different firing patterns, and plasticity of the AHP.

Perhaps the most surprising and important observation made here is that intracellular methylsulphate causes a progressive increase in the R_N and decrease in the fADP of rat CA1 pyramidal neurons. This result occurred under conditions of minimal postsynaptic activity and with both excitatory and inhibitory synaptic activity blocked. This potential recording artifact should be considered in whole-cell recordings using methylsulphate as the main internal anion.

We found that the AHP was stable regardless of the main anion if triggered at a low rate (once every 150 s). Although the AHP is, on average, smaller in KGluc immediately after obtaining whole-cell configuration, the amplitude of the AHP in KGluc remains constant for the duration of the recording. Thus, we find that the AHP in KGluc does not rundown over time and plasticity of the AHP can be studied using gluconate as the main internal anion.

Activity-dependent AHP plasticity *in vitro*

We also found that activity level, in the form of post-synaptic firing, is a crucial determinant of the stability and plasticity of the AHP when the main anion is gluconate. Our data suggest that the reduction of the AHP is activity dependent, rather than a result of passive rundown, in recordings using gluconate. Blockade of hyperpolarization-activated current (I_h) using 20 μM ZD7288 did not block plasticity ($n = 2$ using 20 spike train, data not shown; and $n = 6$ using a 50 spike train for induction, Kaczorowski *et al.* 2003), suggesting that the plasticity we observe here does not share the same mechanism as that reported in CA1 neurons following postsynaptic theta-burst firing (Fan *et al.* 2005). Moreover, pharmacological blockade of the apamin-sensitive I_{AHP} was not sufficient to block induction of AHP plasticity. Taken together, these data suggest that the locus of the plasticity is the sI_{AHP}.

Previous reports have demonstrated that synaptic activation can also induce long-lasting suppression of the sI_{AHP} (Sourdet *et al.* 2003; Melyan *et al.* 2004; Ruiz *et al.* 2005). However, the plasticity reported here differs both in terms of the induction requirements and mechanism. The fact that repetitive postsynaptic theta-burst firing results in an activity-dependent reduction of the AHP (AHP-R), even in the presence of synaptic blockers, suggests that synaptic activation is not a requirement for induction. Even if indirect release of glutamate onto the neurons were to occur as a consequence of background synaptic release (Fan *et al.* 2005), the concentration of kynurenic acid used in our recording solution was likely to be sufficient to antagonize any plasticity via NMDA receptor or metabotropic glutamate receptor activation (Alt *et al.* 2004). We therefore suggest that the both the induction and expression of sI_{AHP} plasticity shown here results from the intrinsic properties of the neuron (i.e. mediated by voltage-gated channels).

Previous studies using sharp-microelectrode recordings in CA1 pyramidal neurons have also demonstrated an enhancement of the AHP (AHP-E) in response to repeated suprathreshold somatic (Borde *et al.* 1995, 2000) or synaptic stimulation (Borde *et al.* 1999; Le Ray *et al.* 2004). We believe that several factors contribute to the induction of AHP-R instead of AHP-E. For example, the previous studies were conducted using sharp-microelectrodes filled with a potassium acetate-based internal solution. The gradual effects of potassium acetate on AHP plasticity and basic membrane properties have gone largely unexplored. Furthermore, work from our laboratory suggests that the stimulation pattern is one crucial determinant for inducing AHP-R in whole-cell recordings, because this plasticity was only observed when the AHP was triggered with theta-burst firing (Kaczorowski *et al.* 2003). We observe the converse (AHP-E) when using 50 Hz trains of action potentials (Kaczorowski *et al.* 2003).

The functional significance of AHP-R differs from AHP-E. Although modulation of the AHP in either direction is thought to influence learning, the direction of the plasticity imparts a specific role to the AHP during learning. Generally speaking, a reduction in the AHP increases neuronal excitability (Baldissera & Gustafsson, 1971; Gustafsson, 1984) and facilitates LTP in CA1 pyramidal cells (Cohen *et al.* 1999; Sah & Beckers, 1996; Stackman *et al.* 2002), which is thought to have a role in learning and memory (Bliss & Collingridge, 1993). Conversely, an enhancement of the AHP may facilitate long-term depression (LTD), an additional mechanism thought to be involved in learning and memory processes. Taken together, the potential for bidirectional control of neuronal excitability through modulation of the AHP may serve to regulate synaptic strength in multiple ways, therefore playing a vital role in learning.

KMeth-induced increase of R_N may mask AHP plasticity

The fact that activity-dependent plasticity (reduction) of the AHP occurs with KGluc, but is masked or reduced by KMeth, may explain why the apparent rundown of AHP shown in previous studies was greater with KGluc than with KMeth (Zhang *et al.* 1994; Velumian *et al.* 1997). In addition, increases in R_N that occur in KMeth may alter the AHP currents measured under voltage clamp, owing both to direct effects on measurement of the I_{AHP} and sI_{AHP}, as well as effects on the voltage and calcium entry that occur during the voltage step to 0 mV used to elicit the I_{AHP} and sI_{AHP} in voltage-clamp experiments.

Consistent with our observed effects of KMeth, another group has shown an activity-dependent enhancement of the AHP, which is observed with sharp microelectrodes and is not observed in whole-cell recordings using KMeth (Borde *et al.* 1995, 1999, 2000; LeRay, 2004). The mechanism underlying the effects of KMeth on AHP plasticity remains unknown. However, it is clear from the present report that KMeth is gradually blocking channels that are available near the resting potential, as evidenced by the gradual enhancement of R_N. There are at least two mechanisms whereby KMeth could alter the expression of AHP plasticity: (1) KMeth may prevent plasticity through inhibition of a crucial molecular component; or (2) KMeth may mask the expression of the plasticity through its effects on R_N. At this point, we have not ruled out either possibility. However, preliminary data suggest that the inhibitory effects of KMeth on plasticity of the AHP can be overcome by using a stronger stimulation protocol (50 spike theta pattern rather 20 spike pattern). In this case, plasticity of the AHP in KMeth is qualitatively similar to that reported here using KGluc (Kaczorowski *et al.* 2002, 2003). In addition, pharmacological and/or synaptic activation of metabotropic kainate receptors has been shown to produce a long-lasting suppression of the sI_{AHP} in recordings with KMeth (Melyan *et al.* 2002, 2004). Similar effects of synaptic stimulation on the I_{AHP} have also been observed in cortical layer V pyramidal neurons (Sourdet *et al.* 2003) and CA1 pyramidal neurons of the hippocampus (Xu *et al.* 2005). Taken together, these data suggest that plasticity of the AHP is probably masked rather than directly blocked by the internal anion methylsulphate.

Implications for plasticity of the AHP *in vivo*

Several studies have demonstrated that the amplitude of the sAHP is inversely related to learning in different tasks. Specifically, the postburst AHP is reduced after trace and delay eyeblink conditioning (Disterhoft *et al.* 1986; Coulter *et al.* 1989; Sanchez-Andres & Alkon, 1991; Thompson *et al.* 1996; Moyer *et al.* 1996, 2000), as well as odour-discrimination learning (Saar *et al.* 1998; Zelcer *et al.* 2006). Furthermore, the reduction of the sAHP in CA1 pyramidal neurons is transient (Moyer *et al.* 1996), which agrees with behavioural data suggesting that the hippocampus is not the long-term storage site for hippocampus-dependent tasks (Kim & Fanselow, 1992; Kim *et al.* 1995; for review see Zola-Morgan & Squire, 1990). These findings suggest that the reduction in the AHP is an important cellular substrate or marker of learning across different tasks, cortical regions and species.

The subcellular mechanism of learning-induced AHP reduction remains unclear, in part due to the fact that it is not currently possible to identify neurons that have been directly altered in response to training. Therefore, the identification of an artificial stimulation protocol that can reproduce a reduction in the AHP in acute brain slice preparations provides a model system through which to better study these alterations. An *in vitro* model facilitates the use of several new approaches to study AHP plasticity: (1) single-cell RT-PCR to identify important changes in protein expression and phosphorylation states in 'trained' *versus* 'untrained' cells (2); dendritic recordings to examine effects of 'training' and AHP plasticity on dendritic integration and synaptic plasticity; and (3) pharmacology to examine the effects of 'training' on intrinsic plasticity, multiple neurotransmitter systems and second messenger systems. Disadvantages remain, however, as the brain slice preparation removes most of the cortical and subcortical inputs that provide information from the environment, which are crucial components for learning. In addition, as shown here, the recording method must be carefully considered in patch-clamp studies (and probably also in microelectrode studies). Nevertheless, the present study is an important first step towards mimicking the AHP reduction observed in response to behavioural training through modulation of intrinsic properties to facilitate the identification of underlying mechanisms.

References

Adams DJ & Oxford GS (1983). Interaction of internal anions with potassium channels of the squid giant axon. *J Gen Physiol* **82**, 429–448.

Aizenmann C & Linden DJ (2000). Rapid, synaptically driven increases in the intrinsic excitability of cerebellar nuclear neurons. *Nat Neurosci* **3**, 109–111.

Alt A, Weiss B, Ogden AM, Knauss JL, Oler J, Ho K, Large TH & Bleakman D (2004). Pharmacological characterization of glutamatergic agonists and antagonists at recombinant human homomeric and heteromeric kainate receptors in vitro. *Neuropharmacology* **46**, 793–806.

Baldissera F & Gustafsson B (1971). Regulation of repetitive firing in motoneurones by the after hyperpolarization conductance. *Brain Res* **30**, 431–434.

Berger TW & Thompson RF (1978). Identification of pyramidal cells as the critical elements in hippocampal neuronal plasticity during learning. *Proc Natl Acad Sci U S A* **75**, 1572–1576.

Bhattacharjee A, Gan L & Kaczmarek LK (2002). Localization of the Slack potassium channel in the rat central nervous system. *J Comp Neurol* **454**, 241–254.

Bhattacharjee A & Kaczmarek LK (2005). For K^+ channels, Na^+ is the new Ca^{2+}. *Trends Neurosci* **28**, 422–428.

Bhattacharjee A, von Hehn CA, Mei X & Kaczmarek LK (2005). Localization of the Na^+-activated K^+ channel Slick in the rat central nervous system. *J Comp Neurol* **484**, 80–92.

Bliss TV & Collingridge GL (1993). A synaptic model of memory: long-term potentiation in the hippocampus. *Nature* **361**, 31–39.

Borde M, Bonansco C & Buno W (1999). The activity-dependent potentiation of the slow Ca^{2+}-activated K^+ current regulates synaptic efficacy in rat CA1 pyramidal neurons. *Pflugers Arch* **437**, 261–266.

Borde M, Bonansco C, de Sevilla F, Le Ray D & Buno W (2000). Voltage-clamp analysis of the potentiation of the slow Ca^{2+}-activated K^+ current in hippocampal pyramidal neurons. *Hippocampus* **10**, 198–206.

Borde M, Cazalets JR & Buno W (1995). Activity-dependent response depression in rat hippocampal CA1 pyramidal neurons in vitro. *J Neurophysiol* **74**, 1714–1729.

Cohen AS, Coussens CM, Raymond CR & Abraham WC (1999). Long-lasting increase in cellular excitability associated with the priming of LTP induction in rat hippocampus. *J Neurophysiol* **82**, 3139–3148.

Collins KD & Washabaugh MW (1985). The Hofmeister effect and the behaviour of water at interfaces. *Q Rev Biophys* **18**, 323–422.

Costa PF, Santos AI & Ribeiro MA (1992). Slow and medium afterhyperpolarizations in maturing rat hippocampal CA1 neurones. *Neuroreport* **3**, 555–558.

Coulter DA, Lo Turco JJ, Kubota M, Disterhoft JF, Moore JW & Alkon DL (1989). Classical conditioning reduces amplitude and duration of calcium-dependent afterhyperpolarization in rabbit hippocampal pyramidal cells. *J Neurophysiol* **61**, 971–981.

Cudmore R, H & Turrigiano GG (2004). Long-term potentiation of intrinsic excitability in LV visual cortical neurons. *J Neurophysiol* **92**, 341–348.

Disterhoft JF, Coulter DA & Alkon DL (1986). Conditioning-specific membrane changes of rabbit hippocampal neurons measured in vitro. *Proc Natl Acad Sci U S A* **83**, 2733–2737.

Disterhoft JF, Wu WW & Ohno M (2004). Biophysical alterations of hippocampal pyramidal neurons in learning, ageing and Alzheimer's disease. *Ageing Res Rev* **3**, 383–406.

Fan Y, Fricker D, Brager DH, Chen X, Lu HC, Chitwood RA & Johnston D (2005). Activity-dependent decrease of excitability in rat hippocampal neurons through increases in I_h. *Nat Neurosci* **8**, 1542–1551.

Foehring RC, Schwindt PC & Crill WE (1989). Norepinephrine selectively reduces slow Ca^{2+}- and Na^+-mediated K^+ currents in cat neocortical neurons. *J Neurophysiol* **61**, 245–256.

Golding NL, Kath WL & Spruston N (2001). Dichotomy of action-potential backpropagation in CA1 pyramidal neuron dendrites. *J Neurophysiol* **86**, 2998–3010.

Gustafsson B (1984). After potentials and transduction properties in different types of central neurones. *Arch Ital Biol* **122**, 17–30.

Haas HL & Konnerth A (1983). Histamine and noradrenaline decrease calcium-activated potassium conductance in hippocampal pyramidal cells. *Nature* **302**, 432–434.

Inoue I, Pant HC, Tasaki I & Gainer H (1976). Release of proteins from the inner surface of squid axon membrane labeled with tritiated N-ethylmaleimide. *J Gen Physiol* **68**, 385–395.

Kaczorowski CC, Cooper DC, Disterhoft JF & Spruston N (2002). Effects of omega-conotoxin on the afterhyperpolarization in hippocampal CA1 pyramidal neurons. *Abstr Soc Neurosci* **340**, 19.

Kaczorowski CC, Disterhoft JF & Spruston N (2003). Differential activity-dependent plasticity of the slow AHP evoked by tetanic vs. theta-burst stimulation in CA1 pyramidal neurons: a role for the hyperpolarization-activated cation conductance. *Abstr Soc Neurosci* **369**, 13.

Kandel ER & Spencer WA (1961). Electrophysiology of hippocampal neurons. II. After-potentials and repetitive firing. *J Neurophysiol* **24**, 243–259.

Kay AR (1992). An intracellular medium formulary. *J Neurosci Methods* **44**, 91–100.

Kim JJ, Clark RE & Thompson RF (1995). Hippocampectomy impairs the memory of recently, but not remotely, acquired trace eyeblink conditioned responses. *Behav Neurosci* **109**, 195–203.

Kim JJ & Fanselow MS (1992). Modality-specific retrograde amnesia of fear. *Science* **256**, 675–677.

Kohler M, Hirschberg B, Bond CT, Kinzie JM, Marrion NV, Maylie J & Adelman JP (1996). Small-conductance, calcium-activated potassium channels from mammalian brain. *Science* **273**, 1709–1714.

Larson J, Wong D & Lynch G (1986). Patterned stimulation at the theta frequency is optimal for the induction of hippocampal long-term potentiation. *Brain Res* **368**, 347–350.

Le Ray D, Fernandez De Sevilla D, Belen Porto A, Fuenzalida M & Buno W (2004). Heterosynaptic metaplastic regulation of synaptic efficacy in CA1 pyramidal neurons of rat hippocampus. *Hippocampus* **14**, 1011–1025.

Madison DV & Nicoll RA (1984). Control of the repetitive discharge of rat CA 1 pyramidal neurones in vitro. *J Physiol* **354**, 319–331.

Madison DV & Nicoll RA (1986). Actions of noradrenaline recorded intracellularly in rat hippocampal CA1 pyramidal neurones, in vitro. *J Physiol* **372**, 221–244.

McEchron MD & Disterhoft JF (1997). Sequence of single neuron changes in CA1 hippocampus of rabbits during acquisition of trace eyeblink conditioned responses. *J Neurophysiol* **78**, 1030–1044.

McEchron MD, Weible AP & Disterhoft JF (2001). Aging and learning-specific changes in single-neuron activity in CA1 hippocampus during rabbit trace eyeblink conditioning. *J Neurophysiol* **86**, 1839–1857.

McKillen HC, Davies NW, Stanfield PR & Standen NB (1994). The effect of intracellular anions on ATP-dependent potassium channels of rat skeletal muscle. *J Physiol* **479**, 341–351.

Melyan Z, Lancaster B & Wheal HV (2004). Metabotropic regulation of intrinsic excitability by synaptic activation of kainate receptors. *J Neurosci* **24**, 4530–4534.

Melyan Z, Wheal HV & Lancaster B (2002). Metabotropic-mediated kainate receptor regulation of IsAHP and excitability in pyramidal cells. *Neuron* **34**, 107–114.

Metz AE, Jarsky T, Martina M & Spruston N (2005). R-type calcium channels contribute to afterdepolarization and bursting in hippocampal CA1 pyramidal neurons. *J Neurosci* **25**, 5763–5773.

Milner B & Penfield W (1955). The effect of hippocampal lesions on recent memory. 80th meeting. *Trans Am Neurol Assoc*, 42–48.

Moyer JR Jr, Power JM, Thompson LT & Disterhoft JF (2000). Increased excitability of aged rabbit CA1 neurons after trace eyeblink conditioning. *J Neurosci* **20**, 5476–5482.

Moyer JR Jr, Thompson LT & Disterhoft JF (1996). Trace eyeblink conditioning increases CA1 excitability in a transient and learning-specific manner. *J Neurosci* **16**, 5536–5546.

Nakajima T, Sugimoto T & Kurachi Y (1992). Effects of anions on the G protein-mediated activation of the muscarinic K^+ channel in the cardiac atrial cell membrane. Intracellular chloride inhibition of the GTPase activity of GK. *J Gen Physiol* **99**, 665–682.

Oh MM, Kuo AG, Wu WW, Sametsky EA & Disterhoft JF (2003). Watermaze learning enhances excitability of CA1 pyramidal neurons. *J Neurophysiol* **90**, 2171–2179.

Otto T, Eichenbaum H, Wiener SI & Wible CG (1991). Learning-related patterns of CA1 spike trains parallel stimulation parameters optimal for inducing hippocampal long-term potentiation. *Hippocampus* **1**, 181–192.

Ranck JB Jr (1973). Studies on single neurons in dorsal hippocampal formation and septum in unrestrained rats. I. Behavioral correlates and firing repertoires. *Exp Neurol* **41**, 461–531.

Rempel-Clower NL, Zola SM, Squire LR & Amaral DG (1996). Three cases of enduring memory impairment after bilateral damage limited to the hippocampal formation. *J Neurosci* **16**, 5233–5255.

Robbins J, Cloues R & Brown DA (1992). Intracellular Mg^{2+} inhibits the IP3-activated IK_{Ca} in NG108-15 cells. [Why intracellular citrate can be useful for recording IK_{Ca}]. *Pflugers Arch* **420**, 347–353.

Robinson DW & Cameron WE (2000). Time-dependent changes in input resistance of rat hypoglossal motoneurons associated with whole-cell recording. *J Neurophysiol* **83**, 3160–3164.

Ruiz A, Sachidhanandam S, Utvik JK, Coussen F & Mulle C (2005). Distinct subunits in heteromeric kainate receptors mediate ionotropic and metabotropic function at hippocampal mossy fiber synapses. *J Neurosci* **25**, 11710–11718.

Saar D, Grossman Y & Barkai E (1998). Reduced after-hyperpolarization in rat piriform cortex pyramidal neurons is associated with increased learning capability during operant conditioning. *Eur J Neurosci* **10**, 1518–1523.

Sah P (1996). Ca^{2+}-activated K^+ currents in neurones: types, physiological roles and modulation. *Trends Neurosci* **19**, 150–154.

Sah P & Beckers JM (1996). Apical dendritic location of slow after hyperpolarization current in hippocampal pyramidal neurons: implications for the integration of long term potentiation. *J Neurosci* **16**, 4537–4542.

Sanchez-Andres JV & Alkon DL (1991). Voltage-clamp analysis of the effects of classical conditioning on the hippocampus. *J Neurophysiol* **65**, 796–807.

Santi CM, Ferreira G, Yang B, Gazula VR, Butler A, Wei A, Kaczmarek LK & Salkoff L (2006). Opposite regulation of Slick and Slack K^+ channels by neuromodulators. *J Neurosci* **26**, 5059–5068.

Schwindt PC, Spain WJ & Crill WE (1992). Effects of intracellular calcium chelation on voltage-dependent and calcium-dependent currents in cat neocortical neurons. *Neuroscience* **47**, 571–578.

Scoville WB & Milner B (1957). Loss of recent memory after bilateral hippocampal lesions. *J Neurol Neurosurg Psychiatr* **20**, 11–21.

Shah M & Haylett DG (2000). Ca^{2+} channels involved in the generation of the slow afterhyperpolarization in cultured rat hippocampal pyramidal neurons. *J Neurophysiol* **83**, 2554–2561.

Sourdet V, Russier M, Daoudal G, Ankri N & Debanne D (2003). Long-term enhancement of neuronal excitability and temporal fidelity mediated by metabotropic glutamate receptor subtype 5. *J Neurosci* **23**, 10238–10248.

Spigelman I, Zhang L & Carlen PL (1992). Patch-clamp study of postnatal development of CA1 neurons in rat hippocampal slices: membrane excitability and K^+ currents. *J Neurophysiol* **68**, 55–69.

Stackman RW, Hammond RS, Linardatos E, Gerlach A, Maylie J, Adelman JP & Izounopoulos I (2002). Small conductance Ca^{2+}-activated k^+ channels modulate synaptic plasticity and memory encoding. *J Neurosci* **22**, 10163–10171.

Stocker M, Krause M & Pedarzani P (1999). An apamin-sensitive Ca^{2+}-activated K^+ current in hippocampal pyramidal neurons. *Proc Natl Acad Sci U S A* **96**, 4662–4667.

Storm JF (1989). An after-hyperpolarization of medium duration in rat hippocampal pyramidal cells. *J Physiol* **409**, 171–190.

Storm JF (1990). Potassium currents in hippocampal pyramidal cells. *Prog Brain Res* **83**, 161–187.

Tasaki I, Singer I & Takenaka T (1965). Effects of internal and external ionic environment on excitability of squid giant axon. A macromolecular approach. *J Gen Physiol* **48**, 1095–1123.

Thomas MJ, Watabe AM, Moody TD, Makhinson M & O'Dell TJ (1998). Postsynaptic complex spike bursting enables the induction of LTP by theta frequency synaptic stimulation. *J Neurosci* **18**, 7118–7126.

Thompson LT, Moyer JR Jr & Disterhoft JF (1996). Transient changes in excitability of rabbit CA3 neurons with a time course appropriate to support memory consolidation. *J Neurophysiol* **76**, 1836–1849.

Velumian AA, Zhang L, Pennefather P & Carlen PL (1997). Reversible inhibition of I_K, I_{AHP}, I_h and I_{Ca} currents by internally applied gluconate in rat hippocampal pyramidal neurones. *Pflugers Arch* **433**, 343–350.

Xu J, Kang N, Jiang L, Nedergaard M & Kang J (2005). Activity-dependent long-term potentiation of intrinsic excitability in hippocampal CA1 pyramidal neurons. *J Neurosci* **25**, 1750–1760.

Zelcer I, Cohen H, Richter-Levin G, Lebiosn T, Grossberger T & Barkai E (2006). A cellular correlate of learning-induced metaplasticity in the hippocampus. *Cereb Cortex* **16**, 460–468.

Zhang L, Weiner JL, Valiante TA, Velumian AA, Watson PL, Jahromi SS, Schertzer S, Pennefather P & Carlen PL (1994). Whole-cell recording of the Ca^{2+}-dependent slow afterhyperpolarization in hippocampal neurones: effects of internally applied anions. *Pflugers Arch* **426**, 247–253.

Zola-Morgan S & Squire LR (1990). The neuropsychology of memory. Parallel findings in humans and nonhuman primates. *Ann N Y Acad Sci* **608**, 434–450; discussion 450–436.

Zola-Morgan S, Squire LR & Amaral DG (1986). Human amnesia and the medial temporal region: enduring memory impairment following a bilateral lesion limited to field CA1 of the hippocampus. *J Neurosci* **6**, 2950–2967.

Acknowledgements

The authors wish to thank Dr Gianmaria Maccaferri and Shannon Moore for their advice and critical reading of the manuscript. Caroline Cook provided advice on the illustrations. This work was supported by the National Institutes of Mental Health grant F31 MH-067445 awarded to C.C.K., and National Institutes of Health grant R37 AG-08796 award to J.F.D. and R01 NS-35180 awarded to N.S.

Supplemental material

The online version of this paper can be accessed at:
DOI: 10.1113/jphysiol.2006.124586
http://jp.physoc.org/cgi/content/full/jphysiol.2006.124586/DC1
and contains supplemental material consisting of two figures.

Supplemental Figure 1. Whole-cell recordings showing noradrenaline-sensitive AHPs are similarly reduced by the Ca^{2+} blocker Cd^{2+}
A, Noradrenaline-sensitive (light blue) and Cd^{2+}-senstive (dark blue) AHPs are similar in recordings with KMeth. Representative example of the AHPs before (dark blue) and after (gray) bath application of Cd^{2+} (200 μM) ($n = 4$). *B*, noradrenaline-sensitive (pink) and Cd^{2+}-senstive (red) AHPs are similar in recordings with KGluc. Representative example of the AHPs before (red) and after (gray) bath application of Cd^{2+} (200 μM) ($n = 4$).

Supplemental Figure 2. Input resistance (R_N) is stable in mouse CA1 neurons in KMeth.
A, Time course and magnitude of R_N in whole-cell recordings of mouse CA1 pyramidal neurons using KMeth ($n = 6$).

This material can also be found as part of the full-text HTML version available from http://www.blackwell-synergy.com